

Real-time phase-selective data acquisition system for measurement of wave phenomena in pulsed plasma discharges

S. J. Sanders, R. A. Stern,^{a)} and P. M. Bellan^{b)}

California Institute of Technology, 128-95, Pasadena, California, 91125

(Received 11 August 1997; accepted for publication 15 January 1998)

A novel data acquisition system and methodology have been developed for the study of wave phenomena in pulsed plasma discharges. The method effectively reduces experimental uncertainty due to shot-to-shot fluctuations in high repetition rate experiments. Real-time analysis of each wave form allows classification of discharges by wave amplitude, phase, or other features. Measurements can then be constructed from subsets of discharges having similar wave properties. The method clarifies the trade-offs between experimental uncertainty reduction and increased demand for data storage capacity and acquisition time. Finally, this data acquisition system is simple to implement and requires relatively little equipment: only a wave form digitizer and a moderately fast computer.

© 1998 American Institute of Physics. [S0034-6748(98)02504-0]

I. INTRODUCTION

The study of transient phenomena in short-lived physical systems, such as pulsed plasma discharges, poses unique experimental challenges. One source of difficulty is that high repeatability of plasma conditions from discharge to discharge is needed in order to allow use of diagnostic instruments which require large data sets to form a complete measurement, i.e., diagnostics which “integrate over” multiple discharges to deduce a given physical quantity. Identical reproduction of a single “pure” plasma on successive shots would, of course, be desirable. Plasma devices are rarely so accommodating, however, and plasma kinetic properties may fluctuate substantially from pulse to pulse due to sensitive dependence on microscopic initial conditions. For example, waves propagating in pulsed plasma discharges may fluctuate in amplitude or in phase (relative to the discharge initiation) from shot to shot. In such cases, any physics which depends on the wave phase can be examined only if diagnostic instruments can be synchronized to the jittering waves. As will be shown, simple averaging over many shots with such phase fluctuations does not alleviate the phase jitter problem.

We have developed a novel data-acquisition system which ensures phase synchronization between waves propagating in pulsed plasma discharges and any plasma diagnostic instruments in use. The principle of this wave-selective data acquisition system (WDAS) is to characterize in real time the phase and amplitude deviation of each discharge wave form relative to a “nominal” wave form. Those shots with wave forms quantitatively similar to the nominal wave form comprise a set with low phase and amplitude scatter, and measurements restricted to those shots are used to diagnose the plasma; data from shots which deviate excessively from the nominal are discarded. This selective data acceptance/rejection method is best suited for high repetition

rate experiments since it reduces the experimental data acquisition rate. However, the method ensures that wave-sensitive measurements are elicited from an essentially pure set of plasmas with well-defined wave structure, rather than from a set having a broad distribution of wave phases and amplitudes.

The WDAS was designed to enable phase-sensitive measurements of plasma ion dynamics in the presence of large-amplitude electrostatic waves in the Caltech Encore tokamak. Although the method was designed specifically for Encore plasmas, it should be well suited for other repetitive experiments with wave phase jitter. Section II discusses the wave fluctuations in the Encore device. Section III presents the details of the new acquisition system. Section IV shows the reduction in phase jitter provided by this new system and briefly describes measurements of fast ion heating cycles obtained through its use. Section V gives additional discussion and concluding remarks.

II. DRIFT WAVES AND PHASE JITTER IN ENCORE PLASMAS

The Encore repetition rate is 15 Hz, with each inductively coupled discharge having lifetime $\tau_{\text{plasma}} \approx 1$ ms. Encore’s toroidal current excites coherent, poloidally propagating electrostatic drift waves¹ with period $T = 230 \mu\text{s}$. Drift waves are a class of normal modes ubiquitously present in inhomogeneous plasmas.² The drift wave growth rate ω_i depends on the plasma density gradient as³

$$\omega_i \propto \left(\frac{1}{n} \frac{\partial n}{\partial r} \right)^2,$$

where n is the plasma density and r is a direction normal to the plasma’s confining magnetic field. Thus, small fluctuations in the plasma density profile can strongly affect the drift wave growth rate. In practice, the spatial profile of gas ionization is not easily controlled in pulsed plasmas. This is the case in Encore, where the drift wave routinely fluctuates by $\pm 15\%$ in amplitude and by $\pm 90^\circ$ in phase from shot to

^{a)}Permanent address: University of Colorado, Boulder, CO 80309.

^{b)}Electronic mail: PBELLAN@CCO.CALTECH.EDU

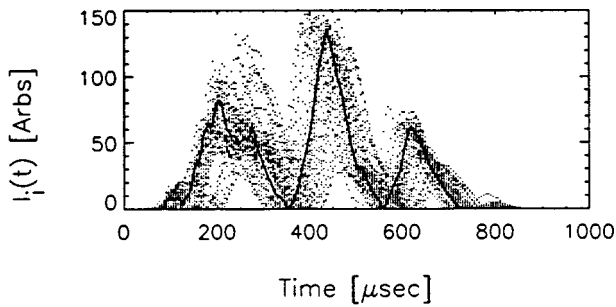


FIG. 1. Fifty ion saturation current traces, showing shot-to-shot jitter in the drift wave phase and amplitude. The time origin is fixed relative to the trigger time of the Ohmic heating pulse.

shot. Examples of the shot-to-shot variations are displayed in Fig. 1. The solid curve shows the ion current collected by an electrostatic probe (inserted near the plasma edge) during one representative shot. The dotted traces are the current wave forms from the next 50 shots.

The large-amplitude drift waves cause fast ion heating and cooling cycles. To observe these rapid heating oscillations, we developed the WDAS to ensure synchronization between the drift wave phase and two multi-shot plasma diagnostics: Langmuir probes⁴ and a pulsed laser-induced fluorescence (LIF) system.⁵ With LIF, a probing laser is scanned across a plasma absorption line to deduce the ion kinetic distribution function, and several thousand plasma shots may be required to obtain the velocity dependence of $f(\mathbf{x}, \mathbf{v}, t)$ at fixed \mathbf{x} and t . Langmuir probe measurements of plasma potential and electron temperature also require multiple shots, since the probe bias must be scanned to obtain the plasma current-voltage characteristic.

To see the difficulty in using multi-shot diagnostics when the plasma suffers from shot-to-shot wave jitter, consider the experimental timing for an LIF experiment, as shown schematically in Fig. 2. Each plasma discharge is initiated by a pulse through the “ohmic heating” (OH) transformer at time t_{OH} . The discharge repetition rate f_{rep} is determined by the Ohmic heating power supply. The figure shows two successive discharges with drift waves out of phase by 180° , corresponding to the extreme limit of the

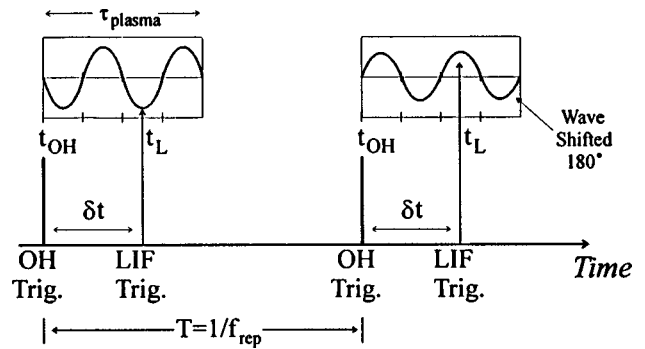


FIG. 2. Layout of experimental timing for LIF measurement in pulsed plasma discharge.

phase fluctuation mentioned above. The wave amplitudes also differ slightly.

Now consider an LIF measurement performed at time t_L . The laser pulse trigger t_L is generated by a programmable delay δt referenced to t_{OH} . The laser pulse width is much shorter than the wave period, so that the LIF signal is a measure of the ion absorption $A_1(t_L)$, where the subscript 1 denotes measurement of discharge 1. During discharge 2 the laser is fired at the *same* delay δt but the wave phase has shifted 180° , meaning that the two successive measurements interrogate exactly opposite wave phases. Clearly if the wave phase continues to fluctuate by exactly 180° from shot to shot, then an ensemble average over many measured samples will “smear” the phases together and destroy the experimental phase resolution. Note that fluctuating wave phase is very different from the case of fluctuating wave amplitude. For fixed phase, random amplitude fluctuations are eliminated by simple averaging, i.e., the ensemble average $\bar{A}(t_L) = N^{-1} \sum A_i(t_L)$ converges to the “true” value of $A(t_L)$, and the rms deviation $[(N-1)^{-1} \sum (\bar{A} - A_{true})^2]^{1/2}$ decreases like $N^{-1/2}$, where N is the number of measured samples. This discussion demonstrates that averaging over fluctuating wave amplitude is permissible but averaging over fluctuating wave phase is not. More precisely, \bar{A} is not an unbiased estimator of A_{true} if the wave phase fluctuates.

A common approach to ameliorate such phase jitter

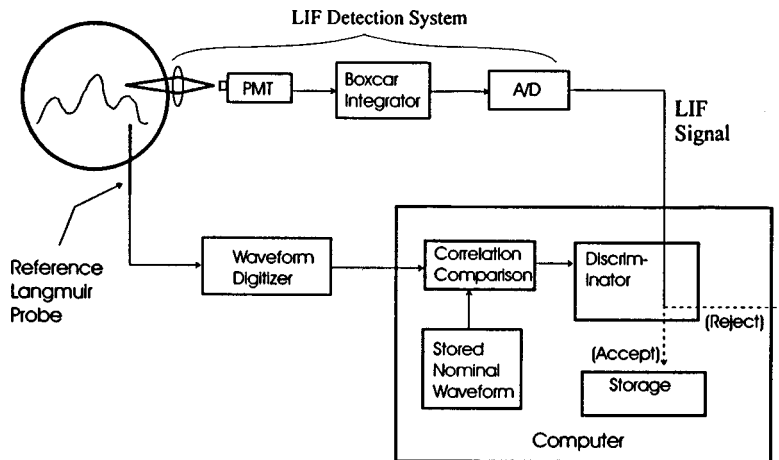


FIG. 3. Schematic of real-time data acquisition system used to select plasmas with low phase jitter.

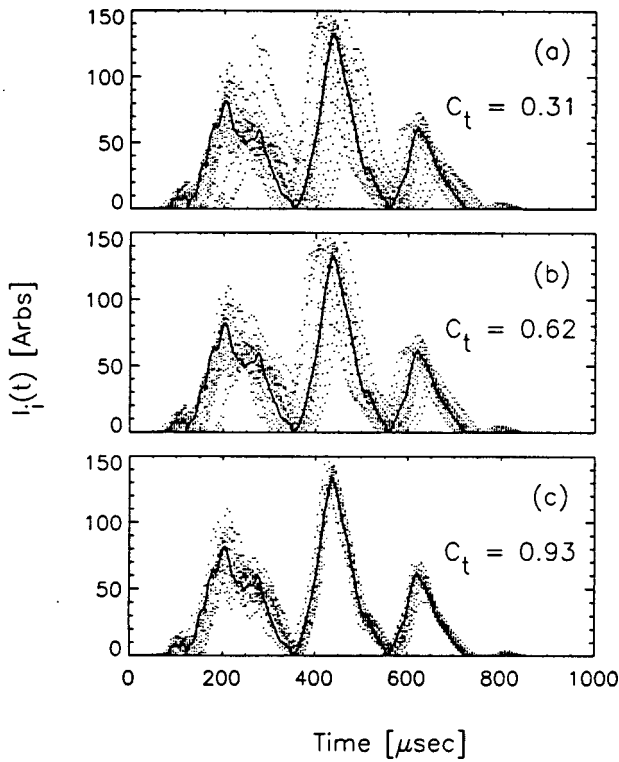


FIG. 4. Sets of ion saturation current wave forms $I_i^{\text{ref}}(t)$ with minimum correlation thresholds shown. The fraction of shots typically exceeding these minimum thresholds is (a) 89%, (b) 76%, and (c) 42%.

problems is to trigger the laser directly on the wave phase by continuously monitoring the phase using a second diagnostic, for example, a Langmuir probe: when the measured wave signal surpasses some predefined threshold, t_L is triggered. However, this method works only if the laser can be triggered in a time short compared to τ_{plasma} . Our LIF system consisted of a Lambda Physik dye laser (model FL2001E) pumped by a Moletron Nd:yttrium-aluminum-garnet (YAG) laser (MY-32). The YAG laser required a 760 μs delay between the flash lamp and Q-switch triggers. Since the plasma lifetime was only about 1000 μs , a phase-triggered flash lamp could easily delay the Q-switch trigger until after the discharge terminated and, moreover, would not allow for interrogation of early wave phases. Also, the observed drift wave jitter of $\pm 50 \mu\text{s}$ was greater than the $\pm 20 \mu\text{s}$ tolerance in the flash lamp Q-switch delay, meaning that the Q-switch trigger could not be directly referenced to wave phase. Therefore, another method of synchronizing the laser trigger to the drift wave phase was needed.

III. WAVE FORM DISCRIMINATION TECHNIQUE

To reduce the experimental uncertainty in drift wave phase and amplitude, we assembled a new data acquisition system which selected in real time plasma discharges with low wave phase and amplitude deviation from a predefined nominal wave form. Discharges with deviation greater than a preestablished threshold were rejected and LIF data from those shots were ignored. Conversely, shots with deviation lower than the threshold were accepted, and LIF data from those shots were used to measure $f(\mathbf{v}, t)$. This method en-

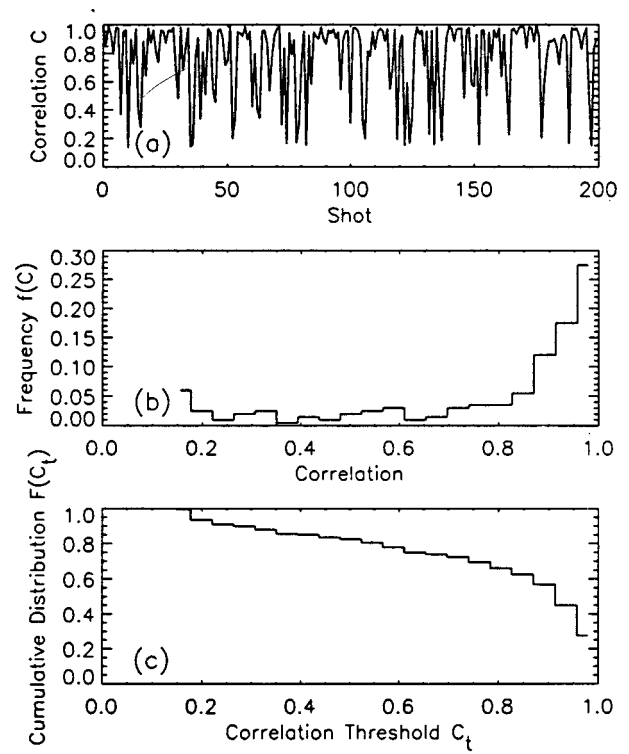


FIG. 5. (a) Scatter plot of measured correlations for 200 consecutive shots. (b) Relative frequency of shots with correlation C . (c) Fraction of discharges with $C \geq C_t$.

sured that the waves used for averaging purposes were selected from a subset of discharges having low phase and amplitude scatter.

The WDAS used the ion saturation current $I_i^{\text{ref}}(t)$ collected by a ‘reference’ Langmuir probe as a measure of the drift wave pattern. Prior to beginning an experiment, a set of 100 such $I_i^{\text{ref}}(t)$ were digitized at a 200 kHz sampling rate (Transiac Model 2008 transient digitizer), and a nominal drift wave form $I_i^{\text{nom}}(t)$ was chosen from among this set, based on its statistical representation within the set. This nominal wave form was stored for comparison to $I_i^{\text{ref}}(t)$ obtained in later shots.

For each shot during an experiment, $I_i^{\text{ref}}(t)$ was digitized, and the data from any other diagnostic, such as the LIF system, were separately digitized (Kinetic Systems ADC 3553) and temporarily stored. The digitized samples of each $I_i^{\text{ref}}(t_k)$ were compared in real time to the stored $I_i^{\text{nom}}(t_k)$ by means of a linear Pearson correlation function;⁶ here t_k refers to the time of the k th digitized sample. With the notation

$$\left\{ \begin{array}{l} R_k = I_i^{\text{ref}}(t_k) \\ N_k = I_i^{\text{nom}}(t_k) \end{array} \right\},$$

the Pearson correlation may be written

$$C(N, R) = \frac{\sum_k (N_k - \bar{N})(R_k - \bar{R})}{\sqrt{\sum_k (N_k - \bar{N})^2} \sqrt{\sum_k (R_k - \bar{R})^2}},$$

where \bar{N} and \bar{R} are the averages of the sequences N_k and R_k . Note that $C=1$ if $N_k=R_k$ for all k , and $C=-1$ if $N_k=-R_k$. For uncorrelated sequences, $C=0$. Thus a value

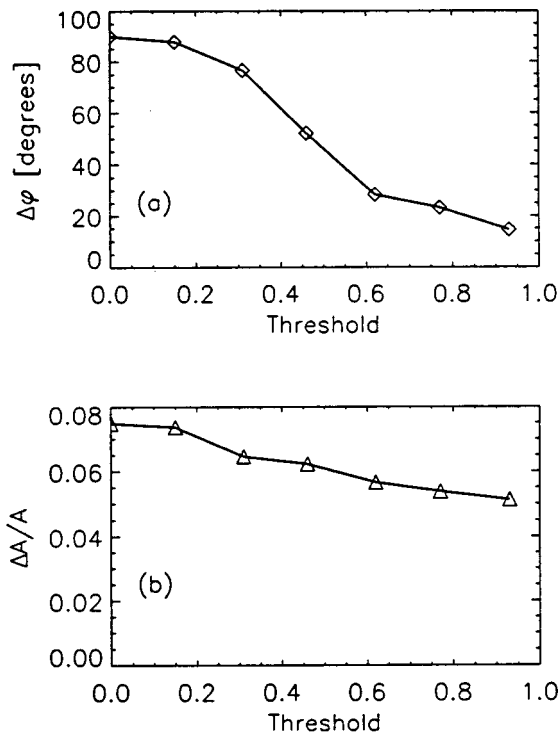


FIG. 6. (a) Measured uncertainty in the drift wave phase (relative to a fixed time origin) as a function of C_t . (b) Relative uncertainty in wave amplitude.

of $C(I_i^{ref}, I_i^{nom}) \approx 1$ indicates good phase and amplitude agreement between a given shot and the nominal wave form. Figure 3 shows a schematic representation of the WDAS setup.

The correlation $C(I_i^{ref}, I_i^{nom})$ was computed in real time for every discharge by a 100 MHz Pentium computer. For discharges with C exceeding the predefined threshold C_t , the stored LIF data were used to compute $f(\mathbf{v}, t)$. For discharges with $C < C_t$, the LIF data were discarded. Typically, $C_t = 0.92 - 0.96$ was used. The 67 ms between discharges was ample time to calculate $C(I_i^{ref}, I_i^{nom})$ and also perform other simple calculations on the LIF data.

IV. IMPROVEMENT IN WAVE JITTER

Typical sets of wave forms selected by this correlation method are shown in Fig. 4, for various thresholds C_t . The nominal wave form $I_i^{nom}(t)$ is the solid curve in each plot. The data in Fig. 4(a) include all shots for which the correlations exceed only $C_t = 0.31$, a very minimal threshold. These data show large phase fluctuations, implying that LIF measurements referenced to t_{OH} sample a wide range of wave phases on successive shots. One expects this phase uncertainty to smear the measured wave structure, as described above. The data in Fig. 4(c) include only those shots with $C \geq C_t = 0.93$; here the phase uncertainty is markedly reduced. In each case, 20 shots are shown. To obtain a set of 20 shots satisfying $C \geq C_t$ for each C_t shown in Figs. 4(a) through 4(c), respectively, the WDAS sifted through 23, 27, and 47 total plasma shots.

Figure 5(a) shows a scatter plot of measured correlations for 200 consecutive shots. These data indicate that the wave phase fluctuates essentially randomly on a shot-by-shot ba-

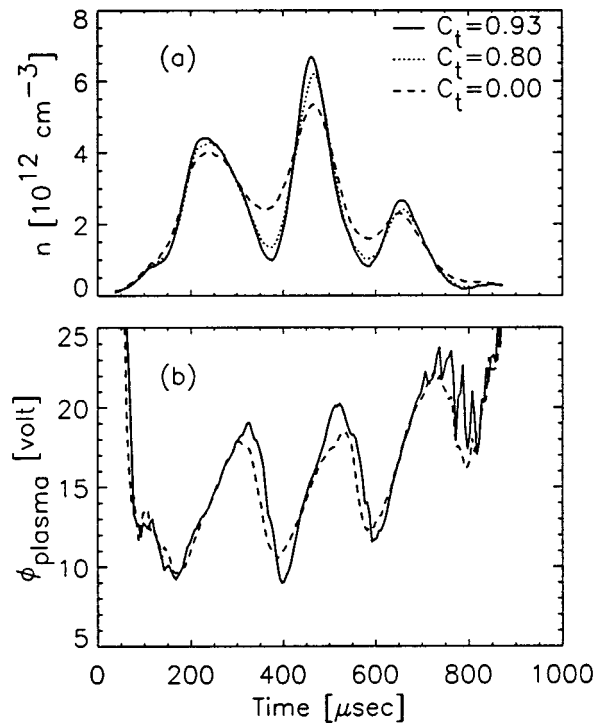


FIG. 7. (a) Ion density and (b) plasma potential obtained from Langmuir probe measurements. The measurement was repeated using a range of C_t , to examine the effect of smearing due to wave phase jitter. $C_t = 0$ corresponds to indiscriminate averaging over all shots. For clarity, the ϕ_p plot shows only two values of C_t .

sis; discharges with similar wave patterns do not occur in bunches. Figure 5(b) shows the probability distribution $f(C)$ of shots with correlation C . The pronounced peak near $C \approx 1$ indicates that the chosen nominal wave form is indeed rep-

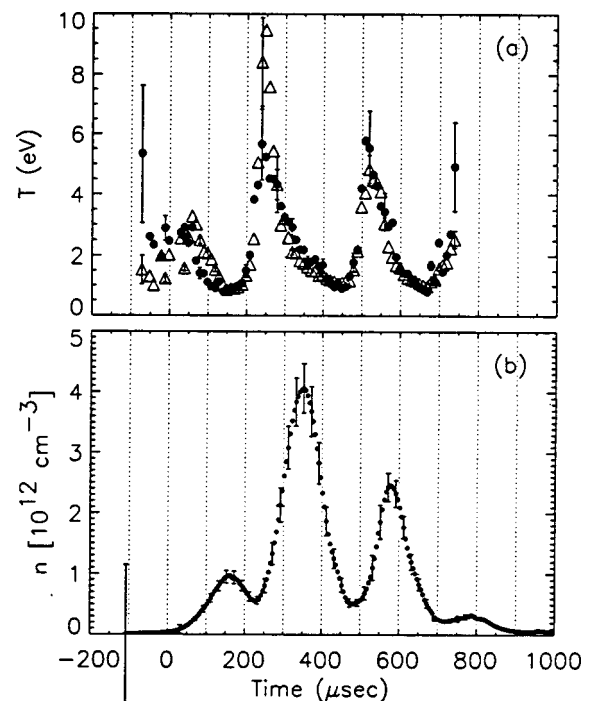


FIG. 8. (a) Two components of ion temperature in the $r-\theta$ plane perpendicular to the magnetic field: T_r (\bullet) and T_θ (Δ). (b) Ion density measured at the same location by a Langmuir probe.

representative of the most probable wave form. Figure 5(c) shows the fraction of discharges with $C \geq C_t$, i.e., $F(C_t) = \int_{C_t}^1 f(C) dC$. This last plot illustrates the obvious disadvantage of the correlation selection scheme: increasing C_t rapidly decreases the frequency of acceptable shots. For example, 77% of typical shots have $C \geq 0.6$, while only 27% have $C \geq 0.95$.

The efficacy of the WDAS in reducing experimental noise can be quantified by tabulating the phase φ of each wave, relative to a fixed time origin. We define $\varphi_i = (t_i^{\text{peak}} - t_{\text{OH}}) / \tau_{\text{wave}}$, where τ_{wave} is the wave period and t_i^{peak} is the time at which $I_i(t)$ achieves its absolute maximum. Typically, $t_{\text{peak}} \approx 430 \mu\text{s}$ (c.f. Fig. 4). Figure 6(a) shows the variance $\Delta\varphi = [(N-1)^{-1} \sum (\varphi_i^2 - \bar{\varphi})^2]^{1/2}$, obtained from an ensemble of $N=80$ wave patterns and acquired using five different values of C_t . Clearly the correlation threshold is a sensitive control of $\Delta\varphi$: by increasing C_t from 0.30 to 0.93, $\Delta\varphi$ decreases from 76° to 14° .

This reduction in phase jitter has a profound effect on measurements made by any of the other Encore diagnostics. As an example, Fig. 7 shows ion density $n(t)$ and plasma potential $\phi_p(t)$, for several values of the acquisition threshold C_t . These data were obtained from a second Langmuir probe located near the LIF ports. One sees that for low C_t , the data are strongly smeared by the effect of averaging over the jittering wave phases, as expected. For instance, use of $C_t=0$ leads one to conclude that the amplitude of the density fluctuations \tilde{n}/n is almost 50% below its true value; similarly, the inferred $\tilde{\phi}_p/\phi_p$ is reduced by 20% from its true value. Using $C_t \approx 0.93$ dramatically reduces the smearing effect.

As an application of the new WDAS, we have used LIF to measure phase-dependent ion velocity distributions in the presence of drift waves with amplitude far above the threshold for stochastic ion heating.⁷ The laser trigger timing was varied to interrogate $f(\mathbf{v}, t)$ in $10 \mu\text{s}$ intervals, and the WDAS ensured that this timing resolution implied high wave phase resolution ($\pm 10^\circ$). Ion temperatures and fluid velocities were then obtained by fitting the measured distributions to Maxwellian distribution functions. Figure 8(a) shows the time evolution of ion temperature for particles located near the tokamak chamber wall. One sees that ions undergo very rapid heating and cooling cycles. These heating cycles are synchronous with, and out of phase with, the wave-induced

density [c.f. Fig. 8(b)] and plasma potential fluctuations. Also, we have observed a phase lag between ion heating perpendicular to and along the toroidal magnetic field B . The physics of this phase lag is beyond the scope of the present discussion of experimental methods, and is presented elsewhere.⁸ We note, however, that these phase relationships would have been severely obscured or perhaps unobservable without the low experimental wave phase uncertainty provided by the WDAS.

V. DISCUSSION

For measurements in Encore, we typically used a data acquisition threshold in the range $C_t = 0.93-0.95$. This value of C_t yielded a good compromise between phase noise reduction (a factor of 5 improvement) and increased data acquisition time (a factor of 2.5 longer). It should be noted that selection of C_t allows optimization of the WDAS for a given set of experimental conditions: the individual experimentalist can decide which operating point along the curve in Fig. 6(a) is most appropriate. In principal, a value of $C_t=0$ could be used, with the reference wave form $I_i^{\text{ref}}(t)$ and all diagnostic data being digitized and stored during every shot for later characterization. In this case the jittering wave phase would allow interrogation of $f(\mathbf{v}, t)$ over a range of wave phases without varying the laser trigger timing, and these could be correlated with the phase *a posteriori*. Such a method would require vast storage capacity but would offer greatly increased data acquisition rate.

ACKNOWLEDGMENTS

The authors thank Frank Cosso for construction of the time-delay generator and other technical assistance. This work was supported by NSF Grant No. PHY-9413046.

¹E. D. Fredrickson and P. M. Bellan, *Phys. Fluids* **28**, 1866 (1985).

²G. Schmidt, *Physics of High Temperature Plasmas* (Academic, New York, 1979), p. 354.

³A. B. Mikhailovskii and L. I. Rudakov, *JETP* **17**, 621 (1963).

⁴I. H. Hutchinson, *Principles of Plasma Diagnostics* (Cambridge University Press, New York, 1987), p. 66.

⁵R. A. Stern and J. A. Johnson III, *Phys. Rev. Lett.* **34**, 1548 (1975).

⁶W. H. Press, B. P. Flannery, S. A. Teukolsky, and W. T. Vetterling, *Numerical Recipes* (Cambridge University Press, New York, 1986), p. 484.

⁷G. R. Smith and A. N. Kaufman, *Phys. Rev. Lett.* **34**, 1613 (1975); J. M. McChesney, P. M. Bellan, and R. A. Stern, *ibid.* **59**, 1436 (1987).

⁸S. J. Sanders, P. M. Bellan, and R. A. Stern (to be published).